www.czasopisma.pan.pl PAN www.journals.pan.pl
Opto-Electronics Review 25 (2017) 41–45

Contents lists available at ScienceDirect

Opto-Electronics Review

journal homepage: http://www.journals.elsevier.com/opto-electronics review

Synthesis of dispersion-compensating triangular lattice index-guiding photonic crystal fibres using the directed tabu search method

F. Karim

Laboratory of Telecommunications, Faculty of Technology, Aboubekr Belkaid University, Chetouane, Tlemcen, Algeria

ARTICLE INFO

Article history:
Available online 20 April 2017

Keywords:
Triangular lattice index-guiding photonic crystal fibre
Dispersion compensation
Directed tabu search
Synthesis

ABSTRACT

In this paper, triangular lattice index-guiding photonic crystal fibres (PCFs) are synthesized to compensate the chromatic dispersion of a single mode fibre (SMF-28) for an 80 km optical link operating at 1.55 μm, by using a directed tabu search algorithm. Hole-to-hole distance, circular air-hole diameter, solid-core diameter, ring number and PCF length parameters are optimized for this purpose. Three synthesized PCFs with different physical parameters are compared in terms of their objective functions values, residual dispersions, compensation ratios and confinement losses.

1. Introduction

Chromatic dispersion of optical fibres is one of the most important parameters for optical communication systems because of its strong influence on high data rate transmission systems. To remedy this problem, specific optical fibres with various dispersion profiles have been proposed for dispersion compensation and optical switching applications; such as chirped fibre Bragg gratings (FBGs) [1–4], dispersion compensating fibres (DCFs) [5,6], photonic crystal fibres (PCFs) [7–9], etc.

Photonic crystal fibres (PCFs) [10,11] consisting of a central defect region surrounded by multiple air holes that run along the fibre length attract much attention in recent years because of unique properties which are not realized in conventional optical fibres. PCFs are divided into two different kinds of fibres. The first one, index-guiding PCF, guides light by total internal reflection between a solid core and a cladding region with multiple air-holes [12,13]. On the other hand, the second one uses a perfectly periodic structure exhibiting a photonic band-gap (PBG) effect at the operating wavelength to guide light in a low index core-region [14,15].

The aim of this work is to synthesize index-guiding PCFs with triangular lattices formed by circular air-holes by the use of the directed tabu search (DTS) method. A comparison between the synthesized PCFs performances will be made to find the best synthesized dispersion-compensating PCF. Our goal is to minimize the chromatic dispersion of an 80 km optical link by placing the synthesized dispersion-compensating PCFs after a single mode fibre (SMF-28) operating at 1.55 μm. For wavelength division multiplexing (WDM) applications, PCFs should provide large negative dispersion values and a negative dispersion slope over a large wavelength range. Our optimization problem consists in the minimization of the residual dispersion over a wavelength range of 100 nm (1.5–1.6 μm).

In this work, the directed tabu search (DTS) is applied for the first time in synthesis and optimization of PCFs physical parameters for dispersion compensation applications. More details about this hybrid method will be presented in Section 2 of this article. We note that a genetic algorithm, combined with a fully vectorial finite-element solver, has been already presented to design PCFs for a broadband dispersion compensation in a generic stretcher–compressor system of an ytterbium fibre laser in Ref. [16].

2. Synthesis of triangular lattice index-guiding PCFs using a directed tabu search

This section deals with synthesis of physical parameters of index-guiding PCFs characterized with triangular lattices and circular air holes. This kind of PCFs is reconstructed with a negative chromatic dispersion that should reduce the positive chromatic dispersion that occurs from a single mode fibre. Let us take an example of a standard SMF-28^{TM} that provides a positive dispersion of 1390.2 ps/nm km at a 1.55 μm wavelength for an 80 km optical link. This fibre has a positive dispersion slope S_0 of 0.092 ps/nm^2 km and a zero-dispersion value at $\lambda_0 = 1.3115$ μm. The SMF-28^{TM} dispersion approximately equals [17]

$$D_{SMF}(\lambda) \approx \frac{S_0}{4}\left[\lambda - \frac{\lambda_0^4}{\lambda}\right]. \quad (1)$$

E-mail address: karim.fethallah@gmail.com

http://dx.doi.org/10.1016/j.opelre.2017.04.006
1230-3402/

Our optimization problem consists, then, in the minimization of a residual dispersion over a wavelength range that extends from $\lambda = 1.5$ μm to $\lambda = 1.6$ μm. The objective function (residual dispersion) can be written as

$$\text{Objective function} = D_{\text{SMF}}(\lambda) \times L_{\text{SMF}} + D_{\text{PCF}}(\lambda) \times L_{\text{PCF}}, \quad (2)$$

where L_{SMF} equals 80 km.

To reconstruct a PCF with a negative dispersion value and a negative dispersion slope, the directed tabu search (DTS) is applied to synthesize four physical parameters of this device: hole-to-hole distance, Λ (or pitch), air-hole diameter, d (or air-filling fraction, d/Λ), solid-core diameter, d_{co} and ring number, N_{r}. We note that the synthesized negative dispersion is obtained for a 1 km PCF length. The SMF-28 positive dispersion value is perfectly compensated at the 1.55 μm wavelength by adjusting the PCF length L_{PCF}, according to the synthesized negative dispersion value and a zero residual dispersion at the operating wavelength.

The directed tabu search (DTS) method has been chosen for synthesis according to their good performances previously demonstrated in Refs. [18,19]. This method has been for the first time described in Ref. [20]. It has been applied to estimate a thermo-optic coefficient and a thermal expansion coefficient of a chirped fibre Bragg grating [19], the hybrid tabu search algorithm has been also used to optimize strain profiles of a sampled Bragg grating [19]. The performances of this method have been compared with those of other hybrid metaheuristics in Refs. [18,19]. DTS has given the best objective function with a minimum evaluation function number. This comparison has proved that DTS is advantageous in higher dimensional systems.

DTS is a memory-based hybrid algorithm, it uses the Adaptive Pattern Search (APS) based on the Approximate Descent Direction (ADD) and the Nelder–Mead (NM) search in its exploration search as neighbourhood-local search strategies to generate trial points. The Nelder–Mead algorithm is used in the DTS intensification part as a local search strategy to refine the best solutions visited so far. A Tabu List (TL) is introduced to save and rank solutions due to their recency and their objective function values. Therefore, some positions in the TL are kept for the best visited solutions, which helps an intensification scheme to refine the search from these best solutions at the final stage. Around each solution saved in the TL, two types of regions are specified in the search space. The first one is a Tabu Region (TR) in which no new trial point is allowed to be generated. The other is a Semi-Tabu Region (Semi-TR) that comprises a surrounding region around TR. The main role of the Semi-TRs is to generate neighbouring trial points in a special way so that returning back to a visited TR is avoided when the trial solution lies inside a Semi-TR.

Fig. 1 illustrates the cross-section of three synthesized triangular lattice solid-core PCFs showing the core and cladding permittivity, ε, distribution. We have chosen only three PCFs, the best optimized, after several simulation trials using the DTS. These PCFs will be compared between them according to their synthesized physical parameters, objective function values, residual dispersions, compensation ratios, PCF-to-SMF length percentages and confinement

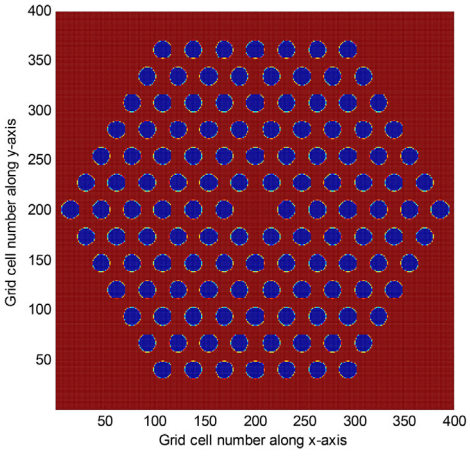

(a) Λ= 0.51 μm; d/Λ= 0.56; d_{co}= 0.73 μm; N_r= 6

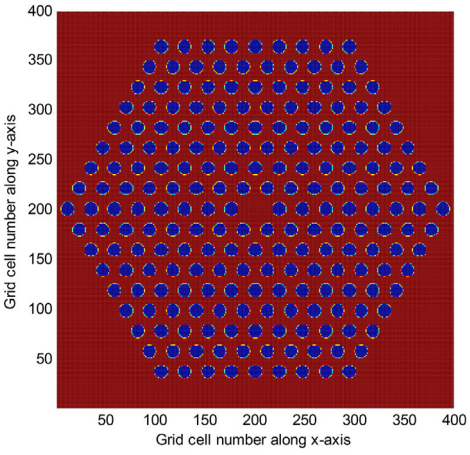

(b) Λ= 0.39 μm; d/Λ= 0.56; d_{co}= 0.56μm; N_r= 8.

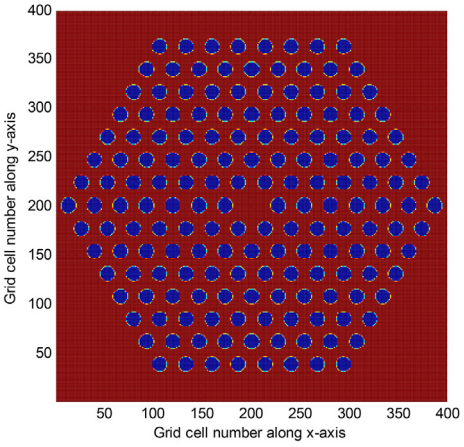

(c) Λ= 0.44 μm; d/Λ= 0.56; d_{co}= 0.63 μm; N_r= 7.

Fig. 1. Core and cladding permittivity distribution of three synthesized triangular lattice solid-core PCFs.

Table 1
Numerical simulation results of three synthesized dispersion-compensating PCFs.

	$\Lambda = 0.51\ \mu m$; $d/\Lambda = 0.5688$; $dco = 0.73\ \mu m$; $Nr = 6$ PCF1	$\Lambda = 0.39\ \mu m$; $d/\Lambda = 0.5641$; $d_{co} = 0.56\ \mu m$; $N_r = 8$ PCF2	$\Lambda = 0.44\ \mu m$; $d/\Lambda = 0.5662$; $d_{co} = 0.63\ \mu m$; $N_r = 7$ PCF3
Objective function value	4.07×10^2	5.90×10^2	6.11×10^2
Residual dispersion at 1.55 μm for 1 km PCF length (ps/nm)	−5.27	3.37	−1.43
Optimized PCF length at 1.55 μm (km)	0.9962	1.0024	0.9989
PCF-to-SMF length percentage at 1.55 μm (%)	1.245	1.253	1.248
Residual dispersion average and maximum error	−1.83/8.83	−1.01/7.25	−3.47/7.18

losses. We note that the air-holes are periodically distributed along the x and y axes and homogeneously distributed along the z-axis. We consider only a Transverse Magnetic (TM) propagation mode, therefore, the electric field E_z is propagating according to the z-axis direction, while the magnetic fields H_x and H_y are propagating along the x-axis and y-axis directions, respectively. We remark from Fig. 1 that the pitch, the air-hole diameter, the solid-core diameter and, consequently, the air-holes' number are different for each synthesized PCF. In our work, the Finite Difference Time Domain (FDTD) method is used for analysis of the PCFs. This method is an approach that directly solves Maxwell's equations by a proper discretization of both time and space domains [21]. Since PCFs are considered as two-dimensional photonic crystals, the PCF cross-section is divided into several grid cells along x and y axes. The grid cell number is taken to 400 along each axis [see Fig. 1], while the total number of time steps equals 4000.

It has been already demonstrated that triangular PCFs are endlessly single mode, where only the fundamental mode is guided for any wavelength, if their air-filling fraction, d/Λ, is lower than 0.406 [22,23]. However, since all synthesized air-filling fractions are higher than this value, it's evident that these PCFs present higher-order modes.

The normalized frequency V is another parameter that determines whether a PCF presents a single fundamental mode or other higher-order modes. This parameter can be written as follows [24]

$$V = \frac{2\pi}{\lambda}\Lambda\sqrt{n_{\text{eff}}^2 - n_{\text{FSM}}^2}, \tag{3}$$

where Λ, n_{eff}, n_{FSM} are the pitch, the effective index of the fundamental guided mode and the effective index of the fundamental space-filling mode (FSM), respectively. A PCF is a single mode, if $V < 2.405$ [17], while it becomes multimode, if $V > 2.405$. It has been shown that in triangular PCFs the second-order mode effective transverse wavelength, related to the dimension of the defect region where the mode fits in, is $\lambda^* \approx 2\Lambda$ at the cut-off condition. As a consequence, the normalized cut-off frequency becomes $V^* = (2\pi/\lambda^*)\Lambda \approx \pi$ [17]. According to the synthesized PCFs apparition order in Fig. 1, the cut-off condition of the second-order mode of the three synthesized PCFs is $\lambda_1^* = 1.02\ \mu m$, $\lambda_2^* = 0.78\ \mu m$ and $\lambda_3^* = 0.88\ \mu m$, respectively.

Table 1 recapitulates the numerical simulation results that concerns the three synthesized dispersion-compensating PCFs already presented in Fig. 1. We note that the apparition order in Fig. 1 is respected in Table 1. We note also that the initial search intervals of the PCF parameters which have been used in the DTS optimization are as follows: $0.6 < \Lambda(\text{pitch}) < 0.9\ \mu m$, $0 < d/\Lambda$ (air-hole diameter to pitch ratio) < 0.6, $1 < N_r$(ring number) < 10 and $0 < d_{\text{core}}$ (core diameter) $< 1\ \mu m$.

It has been demonstrated in Ref. [17] that when the pitch value Λ is lower than 1 μm, the chromatic dispersion value of triangular PCFs is always negative from 1200 nm to 1600 nm. The authors have used Eq. (6) to represent the chromatic dispersion (CD) over the operating wavelength range, where the effective refractive index n_{eff} (which depends on the pitch, the hole diameter, the solid core diameter and the number of rings) was computed through a software code based on the FDTD method, over the same wavelength interval. Since the synthesized hole-to-hole distances values are all lower than 1 μm, the three PCFs present negative dispersion values over the wavelength range of 1.5–1.6 μm. We remind that the aim of this study is to minimize the residual dispersion value over this wavelength range. Since the optical signal attenuation is the lowest at a 1.55 μm wavelength, we will be interested to present the optimized PCFs numerical simulation results at this operating wavelength. For that, we take an SMF of 80 km operating at 1.55 μm (third window).

We remark from Table 1 that DTS has given the lowest objective function value for PCF1, if we place PCF1 after the SMF we still have a residual dispersion of −5.27 ps/nm at 1.55 μm. PCF3 has given the best residual dispersion (−1.43 ps/nm) at the operating wavelength. We note that the PCF dispersion is synthesized for a 1 km PCF length. The residual dispersion will be perfectly minimized at 1.55 μm when the exact PCF length is determined from the residual dispersion relationship as follows

$$L_{\text{PCF}} = D_{\text{SMF}}(1.55) \times L_{\text{SMF}}/D_{\text{PCF}}(1.55) \tag{4}$$

where $L_{\text{SMF}} = 80$ km and $D_{\text{SMF}}(1.55) = 1390.2$ ps/nm.

By using Eq. (4) we find that the corresponding PCF1, PCF2 and PCF3 lengths are of 0.9962 km, 1.0024 km and 0.9989 km, respectively, which gives a PCF-to-SMF length percentage of 1.245%, 1.253% and 1.248%, respectively.

In WDM applications, the positive dispersion and the positive dispersion slope of an SMF should be at the same time compensated by a PCF negative dispersion and a PCF negative dispersion slope. A PCF dispersion slope is considered negative when the slope stays inversely proportional along the whole wavelength range. A triangular PCF presents a positive dispersion slope when its slope curve remains positive starting from a particular wavelength. Therefore, this PCF cannot be used in WDM dispersion compensation the fact that it cannot give the available negative dispersion at each WDM wavelength. To verify this aspect, the compensation ratio (CR) will be calculated. This parameter should be near to 1 over the operating wavelength interval which means that the negative dispersion at each wavelength has been correctly compensated. CR(λ) is the fraction of the SMF dispersion which the PCF compensates at the wavelength λ, that is [17]

$$\text{CR}(\lambda) = \frac{D_{\text{SMF}}(\lambda)}{D_{\text{SMF}}} \times \frac{D_{\text{PCF}}}{D_{\text{PCF}}(\lambda)}. \tag{5}$$

Fig. 2 illustrates the CR plot of the three synthesized PCFs. We remark from this figure that the best compensation ratio is obtained for all reconstructed PCFs at the operating wavelength [CR (1.55) = 1)]. Since PCF1 presents the highest residual dispersion average and maximum error, we remark from Fig. 2 that PCF1 presents the highest CR values when it's compared with PCF2 and PCF3. We note that PCF2 presents the minimum residual dispersion average error over the operating wavelength range.

Fig. 3 illustrates the dispersion curves of the three synthesized triangular lattice solid-core PCFs. We note that the chromatic dis-

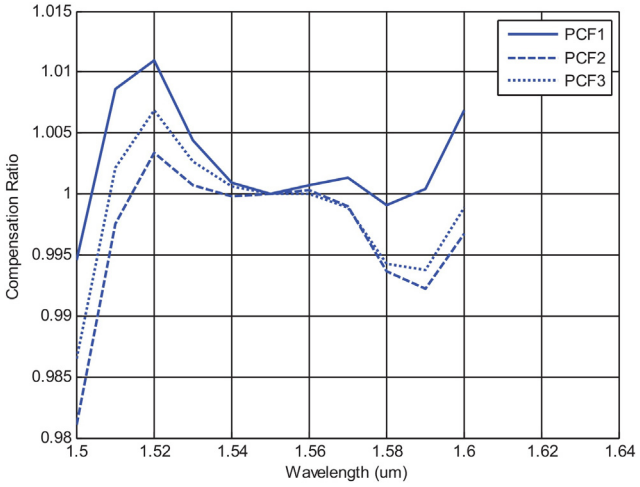

Fig. 2. Compensation ratio of the three synthesized triangular lattice solid-core PCFs.

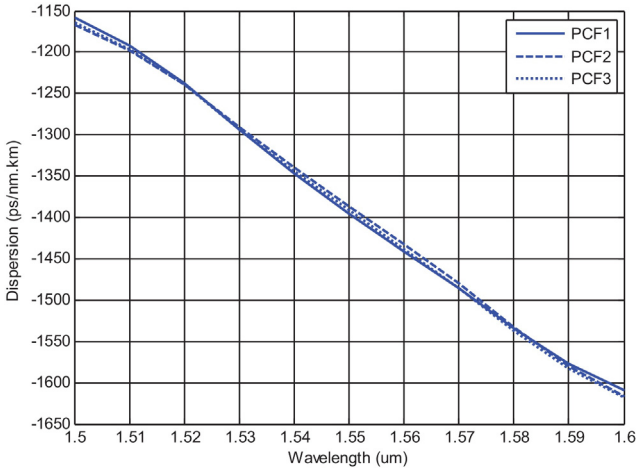

Fig. 3. Dispersion of the three synthesized triangular lattice solid-core PCFs.

persion (CD) is calculated from the real part of the complex effective index, n_{eff}, as [25]

$$\text{CD}(\lambda) = -\frac{\lambda}{c} \times \frac{d^2\, Re(n_{\text{eff}})}{d\lambda^2}, \tag{6}$$

where c is the velocity of light in vaccum.

We remark from Fig. 3 that PCF1, PCF2 and PCF3 present negative dispersion values and negative dispersion slopes over the wavelength range of 1.5–1.6 μm. We can conclude that the three synthesized PCFs are suitable for dispersion compensation in WDM transmission systems.

In solid-core PCFs, light is confined within a core region by the air-holes. Light will move away from the core if the confinement provided by the air-holes is inadequate. This means that it is important to design such aspects of the PCF structure as air-hole diameter and hole-to-hole spacing, in order to realize low-loss PCFs. In particular, the ratio between the air-hole diameter and the pitch must be designed to be large enough to confine light into the core [17]. Fig. 4 presents the confinement loss curves of the three synthesized PCFs. The confinement loss (CL) is calculated from the imaginary part of the complex effective index, n_{eff}, as [25]

$$\text{CL}(\lambda) = 8.686 \times \text{Im}(k_0 n_{\text{eff}}), \tag{7}$$

where k_0 is the free space wave number.

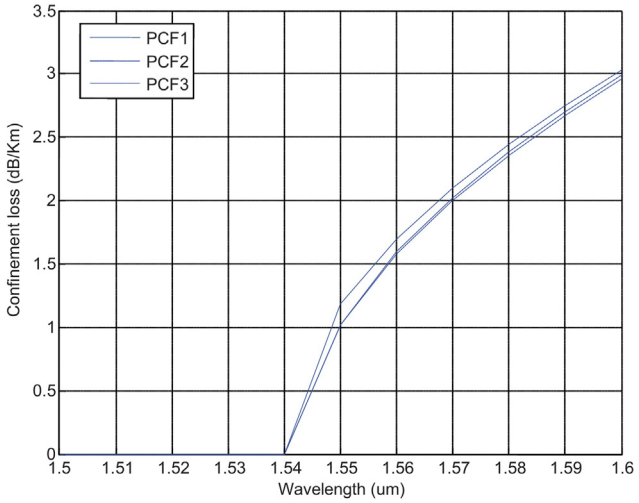

Fig. 4. Confinement loss of the three synthesized triangular lattice solid-core PCFs.

It has been demonstrated in Ref. [17] that the CL quickly decreases when the air-hole ring number, N_r, or the air-hole diameter, d, increases. The reduction rate of the confinement loss increases in the same way with these geometric parameters. We remark from Fig. 4 that PCF2 confinement loss values are little higher than the other PCFs confinement loss ones over the operating wavelength range, because the PCF2 synthesized pitch, Λ, and the core diameter, d_{co}, values are the smallest ones. PCF3 is characterized by the smallest CL values when it's compared with PCF1, because the PCF3 synthesized ring number ($N_r = 7$) is higher than the PCF1 synthesized one ($N_r = 6$). In that case, we note that the ring number impact on the CL reduction rate is much higher than the other parameters impact.

We remark from Fig. 4 that the three synthesized PCFs present acceptable confinement loss values (about an average value of 1.5 dB/km) starting from the 1.54 μm wavelength. We note that the confinement loss is close to 0 dB for the three PCFs from 1.5 μm to 1.54 μm. When the imaginary part of the effective index was computed through the FDTD algorithm over the operating interval of 1.5–1.6 μm, the refractive index took a significant increase starting from 1.54 μm which affected consequently the confinement loss parameter, the fact that the relationship between the two parameters is linear [see Eq. (7)]. The confinement loss can be much more enhanced by increasing the solid core diameter. The appearance of this CL average value between 1.54 μm and 1.6 μm is justified by the small core diameters (less than 1 μm) which characterize the three PCFs. When a PCF core diameter becomes too small, the silica region inside the first ring, in spite of the large surrounding air-holes, is unable to confine the field, which forces an amount of light to propagate outside the solid core.

3. Conclusion

In this paper, three synthesized dispersion-compensating triangular lattice index-guiding PCFs have been compared according to their objective function values, residual dispersions, compensation ratios and confinement losses. The directed tabu search (DTS) has been used to synthesize the pitch, the circular air-hole diameter, the solid-core diameter and the ring number. We note that all synthesized PCFs are not endlessly single mode; they present other higher-order modes according to their cut-off conditions. We note that a PCF-to-SMF length percentage of only 1.25% has been obtained to compensate the chromatic dispersion of an 80 km optical transmission link. In a single mode transmission system centred on 1.55 μm, PCF3 is considered as the best dispersion compen-

sating fibre with a residual dispersion of −1.43 ps/nm km, despite it was reconstructed with the highest objective function value, while PCF2 is the best dispersion compensating fibre in a WDM transmission system because it presents the minimum residual dispersion average error over the whole operating wavelength range of 1.5–1.6 μm. We mention that the three synthesized PCFs present the best compensation ratio (CR = 1) at the 1.55 μm wavelength. We note also that all synthesized PCFs present an average confinement loss value of 1.5 dB/m over the operating wavelength range. Since all synthesized core diameter values are lower than 1 μm, we consider that the confinement loss average value is too high. The confinement loss can be then reduced by increasing the PCF core diameter or the ring number.

References

[1] M. Sumetsky, B.J. Eggleton, Fibre Bragg gratings for dispersion compensation in optical communication systems, J. Opt. Fibre Commun. Res. 2 (2005) 256–278.
[2] Z. Zang, All-optical switching in Sagnac loop mirror containing an ytterbium-doped fibre and fibre Bragg grating, Appl. Opt. 52 (2013) 5701–5706.
[3] Z. Zang, Y. Zhang, Analysis of optical switching in a Yb^{3+} doped fibre Bragg grating by using self-phase modulation and cross-phase modulation, Appl. Opt. 51 (2012) 3424–3430.
[4] Z. Zang, Y. Zhang, Low-switching power (<45 mW) optical bistability based on optical nonlinearity of ytterbium-doped fibre with a fibre Bragg grating pair, J. Mod. Opt. 59 (2012) 161–165.
[5] L. Grüner-Nielsen, et al., Dispersion-compensating fibres, J. Lightw. Technol. 23 (2005) 3566.
[6] P. Palai, A dispersion flattening dispersion compensating fibre design for broadband dispersion compensation, Fiber Integr. Opt. 20 (2001) 21–27.
[7] Y. Ni, et al., Dual-core photonic crystal fibre for dispersion compensation, IEEE Photon. Technol. Lett. 16 (2004) 1516–1518.
[8] Y. Liu, et al., A novel multi-waveband dispersion compensating fibre based on hybrid photonic crystal fibre, Optoelectron. Lett. 9 (2013) 53–56.
[9] M. Mejbaul Haque, et al., Design and characterization of single mode circular photonic crystal fibre for broadband dispersion compensation, Optik – Int. J. Light Electron Opt. 125 (2014) 2608–2611.
[10] J. Broeng, D. Mogilevstev, S.E. Barkou, A. Bjarklev, Photonic crystal fibres: a new class of optical waveguides, Opt. Fibre Technol. 5 (1999) 305–330.
[11] T.A. Birks, J.C. Knight, B.J. Mangan, P.St.J. Russell, Photonic crystal fibres: an endless variety, IEICE Trans. Electron. E84-C (2001) 585–592.
[12] J.C. Knight, T.A. Birks, P.St.J. Russell, D.M. Atkin, All-silica single-mode optical fibre with photonic crystal cladding, Opt. Lett. 21 (1996) 1547–1549.
[13] T.A. Birks, J.C. Knight, P.St.J. Russell, Endlessly single-mode photonic crystal fibre, Opt. Lett. 22 (1997) 961–963.
[14] J.C. Knight, J. Broeng, T.A. Birks, P.St.J. Russell, Photonic band gap guidance in optical fibre, Science 282 (1998) 1476–1478.
[15] R.F. Cregan, B.J. Mangan, J.C. Knight, T.A. Birks, P.St.J. Russell, P.J. Roberts, D.C. Allan, Single mode photonic band gap guidance of light in air, Science 285 (1999) 1537–1539.
[16] R.R. Musin, A.M. Zheltikov, Designing dispersion-compensating photonic-crystal fibres using a genetic algorithm, Opt. Commun. 281 (2008) 567–572.
[17] F. Poli, A. Cucinotta, S. Selleri, Photonic Crystal Fibres: Properties and Applications, Springer, The Netherlands, 2007.
[18] F. Karim, O. Seddiki, Synthesis of chirped apodized fibre Bragg grating parameters using Direct Tabu Search algorithm: application to the determination of thermo-optic and thermal expansion coefficients, Opt. Commun. 283 (2010) 2109–2116.
[19] F. Karim, O. Seddiki, Direct tabu search algorithm for the fibre Bragg grating distributed strain sensing, J. Opt. 12 (2010) 095401.
[20] A. Hedar, M. Fukushima, Tabu Search directed by direct search methods for nonlinear global optimization, Eur. J. Oper. Res. 170 (2006) 329–349.
[21] K. Okamoto, Fundamentals of Optical Waveguides, Academic Press, Elsevier, USA, 2006.
[22] B.T. Kuhlmey, R.C. McPhedran, C.M. de Sterke, P.A. Robinson, G. Renversez, D. Maystre, Microstructured optical fibres: where's the edge? Opt. Express 10 (2002) 1285–1290.
[23] N.A. Mortensen, J.R. Folkenberg, M.D. Nielsen, K.P. Hansen, Modal cut-off and the V parameter in photonic crystal fibres, Opt. Lett. 28 (2003) 1879–1881.
[24] M.D. Nielsen, J.R. Folkenberg, N.A. Mortensen, A. Bjarklev, Bandwidth comparison of photonic crystal fibres and conventional single-mode fibres, Opt. Express 12 (2004) 430–435.
[25] K. Saitoh, M. Koshiba, Chromatic dispersion control in photonic crystal fibres: application to ultra-flattened dispersion, Opt. Express 11 (2003) 843–852.